RUIG: Realistic Underwater Image Generation Towards Restoration

Chaitra Desai Ramesh Ashok Tabib Sai Sudheer Reddy Ujwala Patil Uma Mudenagudi
Centre of Excellence in Visual Intelligence (CEVI), KLE Technological University, Hubballi, Karanataka, INDIA
chaitra.desai@kletech.ac.in, ramesh_t@kletech.ac.in, saisudheer0204@gmail.com,
ujwalapatil@kletech.ac.in, uma@kletech.ac.in

Abstract

In this paper, we present a novel method for generating synthetic underwater images considering revised image formation model. We propose to use the generated synthetic underwater images to train a conditional generative adversarial network (CGAN) towards restoration of degraded underwater images. Restoration of degraded underwater images using traditional dehazing models is challenging as they are insensitive to wavelength, depth, water type and treat backscattering and direct signal attenuation coefficients to be equal. However, learning based models for restoration perform well but sensitive to availability of ground truth information. Generating ground truth labels in underwater scenario demands in-situ measurements using expensive equipments and is infeasible due to varying underwater currents. Towards this, we propose to generate synthetic underwater images using revised image formation model. Revised image formation model is sensitive to different attenuation coefficients: 1) back scattering, 2) direct scattering and 3) veiling light. We propose to estimate these attenuation coefficients considering proven facts from the literature. We demonstrate restoration of real underwater images through restoration framework trained using rendered synthetic underwater images, and compare results of restoration with state-of-the-art techniques.

1. Introduction

In this paper, we propose a framework for generation of synthetic underwater images considering revised image formation model [1] and use the same to train conditional generative adversarial networks, towards restoration of degraded underwater images. Capturing of underwater scene, heavily relies on unmanned vehicles (UV) equipped with imaging sensors, to provide a high-resolution view of sea bed, corals and archaeological sites. Marine archaeologists use the remotely operated vehicle (ROV) to explore the ocean without physically being present in the ocean [12]. Recently, we observe considerable advancement in underwater scene capturing technologies. However, the aquatic environment still presents unique challenges, unlike the above-water environment. Due to light attenuation, absorption and scattering most of the underwater images lack in contrast and depict inaccurate colors. The attenuation of light in water varies with wavelength and depends on its distance, unlike the terrestrial images where attenuation is assumed to be spectrally uniform. Wavelength-dependent attenuation causes color distortion that increases with the distance of an object from the camera. This phenomenon causes underwater images to appear bluish or greenish in color, unlike the above water scene.

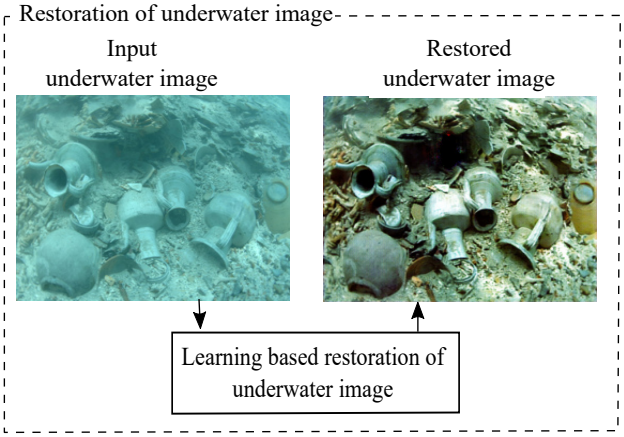

Figure 1. Restoration of underwater images.

Recently, authors propose to use calibrated stereo cameras [11] with improved depth information [5] for 3D reconstruction [13] of underwater archaeological sites. However, with dynamically varying environmental conditions, underwater restoration and 3D reconstruction of submerged sites remain unsolved. Images captured in deep oceanic water have a different distribution of optical properties from those captured in shallow coastal waters. This problem is due to the varying lighting conditions and suspended particles. In deep oceanic water, the penetration of natural light is absolutely nil. Capturing images in artificial light introduces ar-

tifacts causing (certain number of pixels to reach) saturation and limiting the underwater scene's visibility. In shallow coastal water, the suspended particles are more significant than the incident light resulting in non-selective scattering. The non-selective scattering accounts for the formation of haze, limiting the visibility of an underwater scene. In each of these cases, either ocean bed or coastal bed restoration is the need of the hour, towards improved underwater object detection, mapping and tracking of coral reefs and for preserving underwater ecology. Several authors have proposed learning and non learning based techniques towards restoration of underwater images.

Non learning-based methods consider brightest pixel to estimate the veiling light. Tan *et al*. [30] choose brightest pixel and Fattal *et al*. [4] used it as an beginning conjecture. Intuitively, the brightest pixel might not directly contribute towards estimation of veiling light, as the brightest pixel may also belong to object under consideration. To overcome this, He *et al*. [7] choose the the brightest pixel based on the local patches, considering intensities being close to zero in dark channel and determining atmospheric light from haze opaque regions of dark channel. These methods are sensitive to discernible regions of an image and demands to choose hand crafted features towards estimation of attenuation coefficients.

Alternatively, deep neural networks provide the solution for modelling complex non-linear structures. However, deep learning-based solutions are data-dependent and require a large amount of data for training. Learning-based approach for restoration and 3D reconstruction of underwater images remains unsolved unlike the terrestrial applications. Major challenges in deep learning-based architectures are the need for a larger database coupled with labels or corresponding ground truth information. Generating ground truth labels in underwater scenarios demands in-situ measurements using expensive equipment [29]. Performing in-situ measurements requires skilled personnel to handle complex equipment and is a challenging affair. Gathering larger chunks of data with corresponding depth and ground truth information in the underwater scenario is quite challenging and remains an open problem.

Towards this, we propose to generate realistic underwater images considering a revised image formation model and use the same as training data, for learning-based models. Typical image formation model, is derived from atmospheric dehazing equation and are insensitive to wavelength dependencies, resulting in significant errors while restoring/enhancing underwater images. The backscattered signal, is the primary reason for underwater image degradation, and is affected by the scattering and absorption of light, which are wavelength-dependent. There is a need for an image formation framework that incorporates wavelength dependencies, derived from the laws of physics.

We plan to generate synthetic underwater images considering depth [20], wavelength-based attenuation coefficients and several other parameters, we term the algorithm as Realistic Underwater Image Generation (RUIG). Unlike the deep learning algorithms [18], our model is data independent. Authors in [18] propose generative adversarial networks considering on-air images and corresponding depth information to render synthetic underwater images. In proposed model (RUIG) we consider the revised image formation model and the wavelength-based attenuation coefficients to render synthetic underwater images. The generated synthetic underwater images and the corresponding on-air images are used to train conditional adversarial networks (CGAN) [19]. CGAN learns the mapping from synthetic underwater images to on air images towards restoration of degraded underwater images.

Towards this, we propose to address data insufficiency challenges faced by learning-based models for restoration of underwater images, in particular

- We propose to design conditional generative adversarial networks (CGAN) towards restoration of degraded underwater images.
- We propose to generate realistic underwater images using revised image formation model as given by [1] using coefficients of Jerlov water types [29].
- We demonstrate the results of restoration using synthetic and real dataset, and compare the performance of restoration model with state-of-the-art techniques using quantitative metrics.

In Section 2, we present the evolution of image formation model. In Section 3, we discuss the proposed methodology for generation of synthetic underwater images. Methodology for restoration of underwater images is given in Section 4. We demonstrate the results of the proposed methodology in Section 5 and compare the same with state-of-the-art techniques. In Section 6, we discuss conclusions drawn towards the research carried out.

2. Underwater image formation

Fundamental problem in underwater vision is image restoration which aims at recovering a high-quality image from low quality observations. Several image restoration algorithms are proposed to improve the performance. Traditional algorithms use hand crafted features or prior [32, 9] to recover high quality observations from degraded samples. With the advent of deep learning algorithms, restoration has achieved a promising result for on air images. However, restoration in underwater scenario is an open problem as degradation is sensitive to wavelength and depth. Deep learning algorithms are data dependent and capturing data

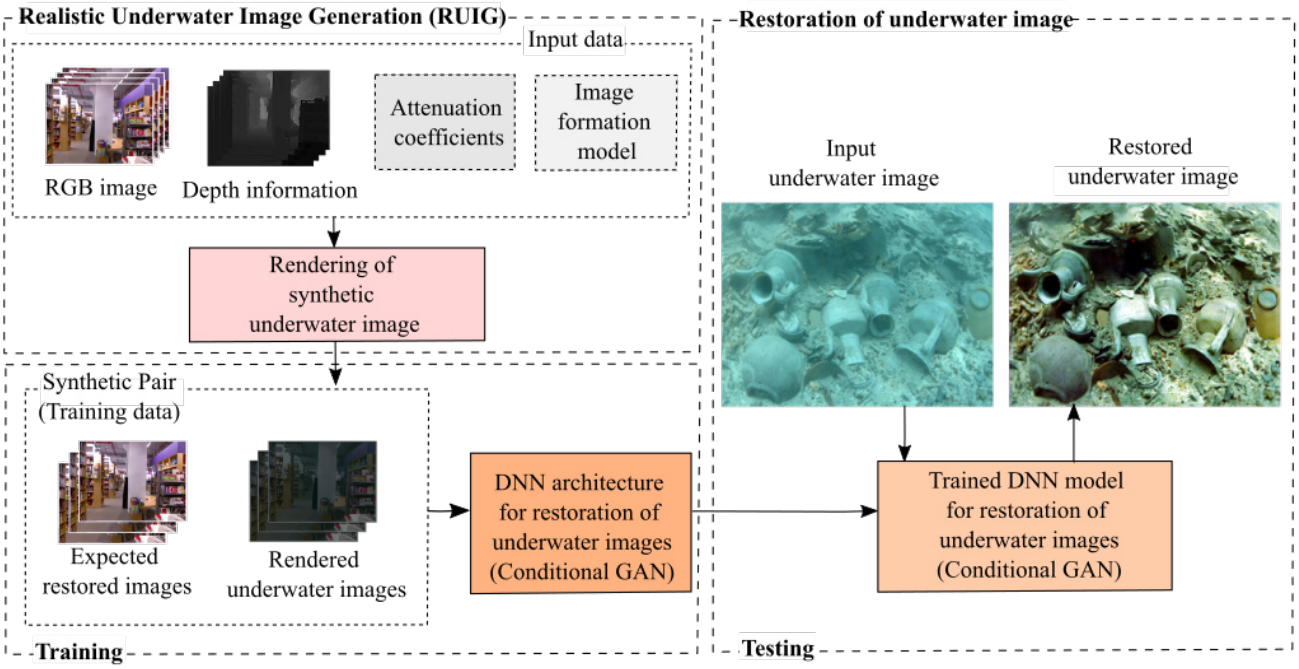

Figure 2. Overview of the proposed framework for realistic underwater image generation towards restoration, includes, realistic underwater image generation (RUIG), training CGAN using the generated synthetic images and, testing the trained model with real underwater images.

in underwater scenario is challenging due to light attenuation and dynamically varying conditions. Towards this, we propose to generate synthetic data modelled using revised image formation model. Generated synthetic data is used to train conditional adversarial networks towards restoration of underwater images.

Authors in [15] and [16] use standard model for both dehazing and restoration of underwater images. The standard model for restoration and dehazing is given as:

$$I(x) = J(x)t(x) + A(1 - t(x)) \tag{1}$$

where $J(x)$ is true scene radiance, $t(x)$ is the transmission and A is the veiling light. The transmission map $t(x)$ through the water medium is given by,

$$t(x) = e^{-\beta_\lambda d(x)} \tag{2}$$

As depicted in Equation 1 and Equation 2 there are three unknown parameters $\{A,\ d(x),\ \beta_\lambda\}$ to be estimated towards restoration of underwater images. Traditional model as given in Equation 1 considers wide band attenuation coefficient β_λ to be spectrally uniform for backscattering and direct attenuation across R, G, B channels. However, authors in [3] demonstrate space of attenuation coefficients as independent entities and represent the same graphically as per 10 Jerlov classes [10].

In underwater scenario propagation of light is influenced by direct light, forward scattering light, and backscattering light. The total light reaching the camera from the object is represented as:

$$I_\lambda = D_\lambda + B_\lambda + F_\lambda \tag{3}$$

where I_λ is the total irradiance received by the camera, B_λ is the backscattered light, D_λ is the direct light, F_λ is forward scattering component respectively. The subscript λ represents the wavelength of color channels R, G and B for an RGB image. However, authors in [28] show quantitatively $F_\lambda \ll D_\lambda$, and it does not contribute significantly to the degradation of an image. Therefore, Equation 3 can be represented as:

$$I_\lambda = D_\lambda + B_\lambda \tag{4}$$

B_λ and D_λ given in Equation 3 can be represented using attenuation coefficients β_c^B and β_c^D (wide band attenuation coefficients) respectively. Rewriting Equation 1 considering wideband attenuation coefficients,

$$D_\lambda = J(x)e^{-\beta_c^D(v_D)d(x)} \tag{5}$$

$$B_\lambda = B_c^\infty(1 - e^{\beta_c^B(v_B)d(x)}) \tag{6}$$

$$I(x) = J(x)e^{-\beta_c^D(v_D)d(x)} + B_c^\infty(1 - e^{\beta_c^B(v_B)d(x)}) \tag{7}$$

where $v_D = \{d(x),\ \rho,\ E,\ S_c,\ \beta\}$ and $v_B = \{E,\ S_c,\ \beta,\ b\}$. Here $d(x)$ is the depth, ρ is the reflectance of each object in the scene, S_c is the spectral response of the camera, E

is the spectral irradiance of the scene, b and β are beam attenuation coefficients.

In what follow, we discuss these parameters β_c^D, β_c^B, and B_c^∞.

2.1. Direct signal (β_c^D)

Scattering involves redirecting the photons away from the line of sight by suspended particles. Signal leaving the camera (Divers Position) hitting the object and reaching back the camera constitutes direct signal. Direct signal carries most information from the scene. However, the phytoplankton's, chlorophyll content, micro-organisms and dissolved organic matter decreases the strength of the signal resulting in direct signal scattering. As depicted in Equation 7 first part of the equation constitutes for true scene reconstruction. Direct signal is greatly influenced by the distance between the object and the camera (Divers Position). Generating accurate depth along with scene information is challenging in underwater scenario. Towards this we consider NYU depth dataset [21] comprising indoor scenes captured using Microsoft Kinet. We have the true scene radiance $J(x)$ and corresponding depth information $d(x)$ for generating synthetic underwater images. Attenuation coefficient representing direct signal scattering is β_c^D and is strongly governed by $d(x)$, ρ, E, S_c, β and is given by authors in [2]. For simplicity we assumed ρ = E = 1 and λ_1 = 400nm and λ_2 = 700nm (Visible spectrum range). We consider spectral response of camera Nikon D90 as given by authors in [6]. We simulate β_c^D considering Equation 8. Figure 3 shows increasing behaviour of β_c^D, as we move from ocean water to coastal bed along the line of turbidity. Increase in turbidity here is influenced by water type and depth $d(x)$.

$$\beta_c^D = \frac{\int_{\lambda_1}^{\lambda_2} S_c(\lambda)\rho(\lambda)E(\lambda)e^{-(\beta(\lambda)d(x)}d(\lambda)}{\int_{\lambda_1}^{\lambda_2} S_c(\lambda)\rho(\lambda)E(\lambda)e^{-(\beta(\lambda)d(\Delta(x))}d(\lambda)} \quad (8)$$

where $\Delta(x)$= x_2 - x_1, all other measurements at the surface are considered in-line with the authors in [2].

2.2. Backscattering signal (β_c^B)

In previous section, we discussed on calculating direct signal as given in Equation 8. Here, in this section we focus on simulating backscattering attenuation coefficient β_c^B. Backscattering is fundamentally governed by the water constituents, the size of the submerged particles and the chlorophyll concentration of the water. Photons (Incident Flux) travelling from the natural source of light, towards the camera (Divers Position) get deflected in all the directions due to floating particles in the water. These photons do not carry any information of the scene and creates a hazy layer. This phenomenon is termed as, backscattering and is primarily responsible for haze formation. The deflection of photon,

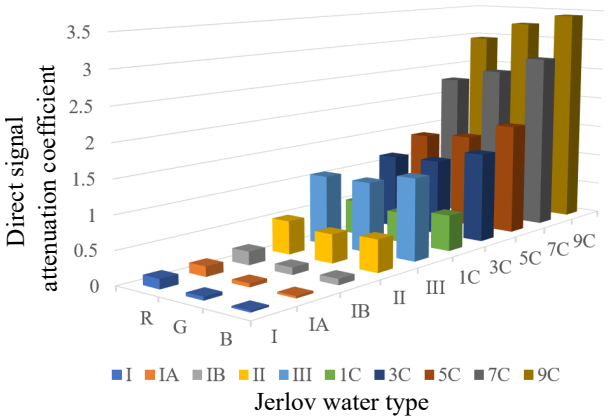

Figure 3. Simulated direct signal attenuation coefficient (β_c^D) across R, G, B channels (visible spectrum). Figure depicts increase in direct signal attenuation for coastal bed compared to ocean water due to increased turbidity. Type (I, IA, IB, II, III) represents ocean bed, and Type (1C, 3C, 5C, 7C, 9C) represents coastal bed.

away from the incident direction is determined by volume scattering function (VSF). However, estimating VSF of a specific ocean water or a coastal bed is possible with in-situ experiments using specialized equipments and a skilled personnel. The measurements associated with 10 water types are given by authors in [10]. For surface measurements, we consider CIE D65 standard values as given by authors in [1].

We simulate β_c^B as given by authors in [2]. β_c^B strongly depends on E, S_c, $\beta(\lambda)$ and $B^\infty(\lambda)$. Few measurements are taken from authors in [29]. Considering all the measurement, we calculate backscattering attenuation coefficient as given by authors in [2]. Estimates of β_c^B is used in revised image formation model as given in Equation 7 towards generation of synthetic underwater images.

2.3. Veiling light (B_c^∞)

In this section, we simulate calculation of veiling light towards synthetic data generation. Natural light gets attenuated with vertical depth before reaching the actual scene and often fails to reach beyond $20m$ - $30m$ depth. Capturing scene beyond $20m$ depth demands artificial source of light, to mimic the behaviour of natural light. Artificial source of light mounted over divers headset is unstable due to ocean and sea currents leading to absorption and scattering. Restoration of lost information due to scattering and absorption is the key towards success of underwater imaging. Towards this, we calculate B_c^∞ as given by authors in [1] and use the estimates in revised image formation model for synthetic underwater image generation.

3. Realistic underwater image generation (RUIG)

In this section, we consider the deliberated values of wide band attenuation coefficients and use it in revised image formation model towards synthetic data generation.

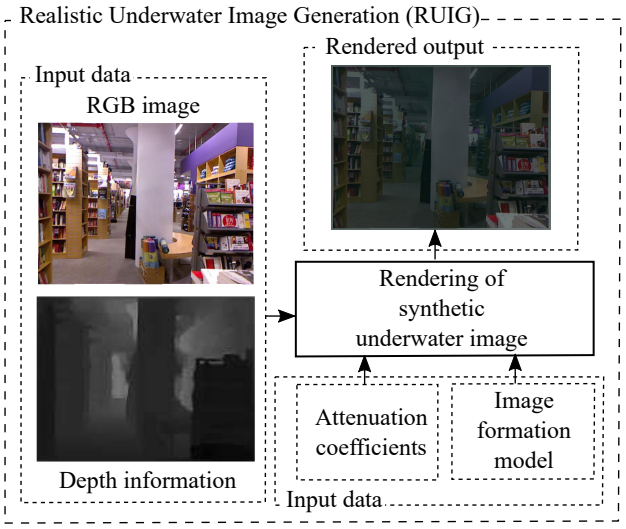

Figure 4. Generation of synthetic underwater images considering wide band attenuation coefficients, True scene radiance $J(x)$ corresponding depth information $d(x)$ as per Revised Image Formation Model.

As shown in Figure 4 we propose to model synthetic data generation considering revised image formation model depicted in Equation 7. NYU depth data set provides R, G, B data and its corresponding depth information. We design an algorithm, that takes true scene radiance $J(x)$ and its corresponding depth $d(x)$ as input, with the deliberated wide band attenuation coefficients. Unlike, the traditional image formation we estimate β_c^D as given in Equation 8 and β_c^B as given by authors in [2] for each color channel R, G, B across visible spectrum range. We generate, 800 images for 10 classes of Jerlov water types across 20 vertical depths. Total of 1,60,000 synthetic underwater images are generated towards training restoration framework. Generated synthetic underwater images are depicted in Figure 6 (Column 1) and Figure 7 (Column 1) respectively, for 10 classes of Jerlov water types.

4. Learning based restoration of underwater images

Generative networks learn mapping from random noise z to output y, however, conditional generative networks learn mapping conversely i.e from input image x and random noise z to output y. Here, we model conditional generative networks to learn mapping from degraded image $x^{'}$ and noise z to ground truth image x i.e $(x^{'} \& \ z) \rightarrow x$. We model $x^{'}$ as our degraded observation and x being the ground truth image and learn the mapping from degraded image to ground truth image towards restoration.

Towards this, we model loss function for conditional generative networks as per Equation 9.

$$L_{CGAN}(G, D) = logD(x^{'}, x) + log(1 - D(x^{'}, G(x^{'}, z))) \quad (9)$$

We model generator with skip connection as given by authors in [27] to learn low frequency components with more detailing. Discriminator is modelled as simple classifier to differentiate between degraded image $x^{'}$ and true image x. Generator and discriminator are modelled with the structure (conv2D $\rightarrow$ batch normalization $\rightarrow$ relu). We use adam optimizer with learning rate of 0.0001.

5. Results and discussions

In this section, we present results of the proposed methodology quantitatively and compare the same with state-of-the-art techniques.

a) Ground truth b) Corresponding depth image

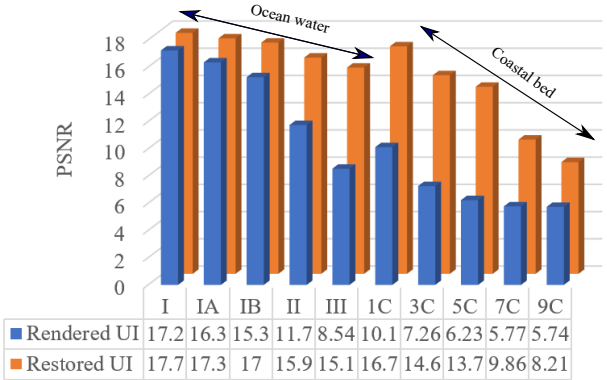

	I	IA	IB	II	III	1C	3C	5C	7C	9C
Rendered UI	17.2	16.3	15.3	11.7	8.54	10.1	7.26	6.23	5.77	5.74
Restored UI	17.7	17.3	17	15.9	15.1	16.7	14.6	13.7	9.86	8.21

Figure 5. The plot for PSNR considering (a) as ground truth (from NYU-Depth dataset). Blue color represents PSNR values for rendered synthetic underwater images, and orange color represents PSNR values of restored underwater images for ocean and coastal beds shown in Figure 6 and 7.

Figure 6. Synthetic underwater image rendered using NYU Depth data set considering Equation 7 and corresponding restored images. First column shows rendered underwater images for ocean water (Type I, IA, IB, II, III) as per Jerlov [10]. Second column shows corresponding restored underwater images using proposed pipeline.

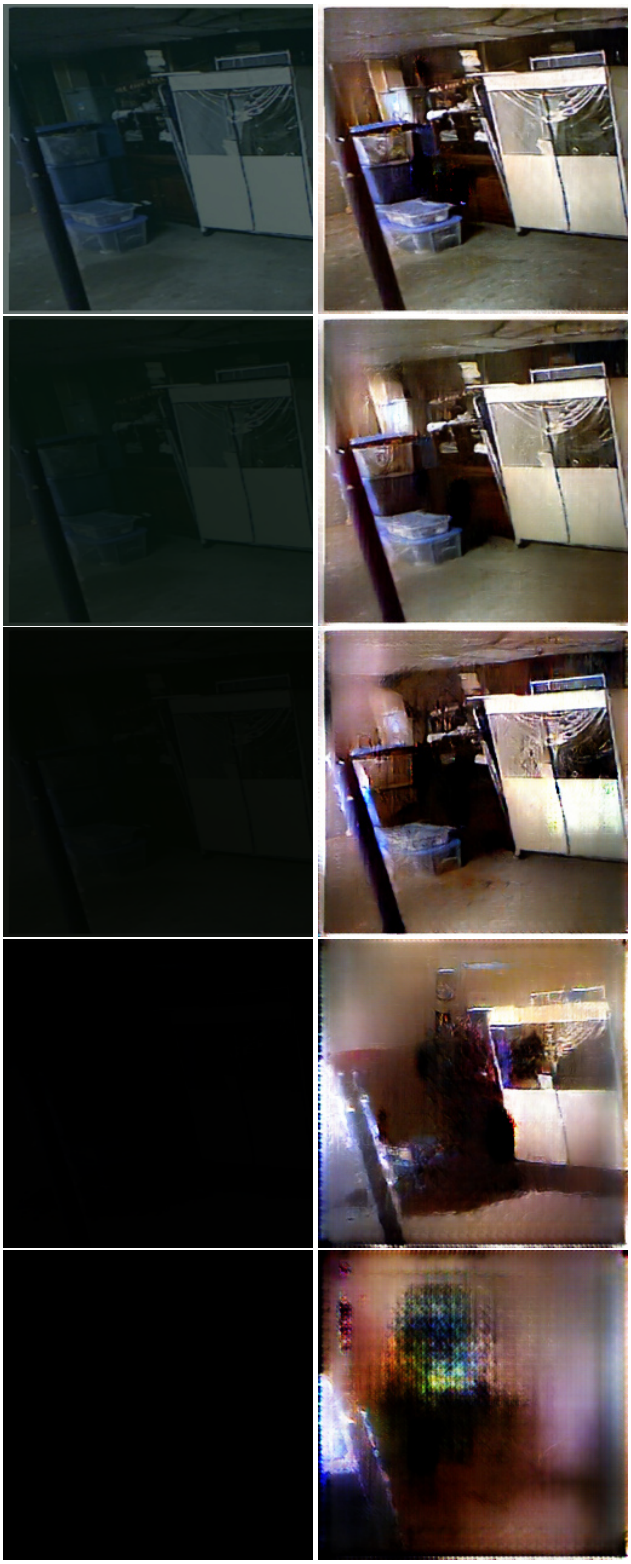

Figure 7. Synthetic underwater image rendered using NYU Depth data set considering Equation 7 and corresponding restored images. First column shows rendered underwater images for coastal beds (Type 1C, 3C, 5C, 7C, 9C) as per Jerlov [10]. Second column shows corresponding restored underwater images using proposed pipeline.

5.1. Quantitative metrics

Quality of the restored image is sensitive to colourfulness, contrast, sharpness and fogginess. Typically qualitative and quantitative analysis is carried out to demonstrate the quality of the restored image. Qualitative analysis is perceptual [23], quantitative quality is carried out as no reference [8] and reference measures. Researchers don't appreciate with reference quality metric as it demands for ground truth information [26] [24] [25]. Towards this, we propose to use no reference quantitative metrics like UCIQE, UIQM and CCF. These metrics depends on the underlying dataset and is a weighted combination of colourfulness, sharpness and contrast. Table 1 shows comparison of our results with state-of-the-art technique [14]. We demonstrate results of proposed methodology using UCIQE [33], UIQM [22] and CCF [31] and prove our restoration results are promising quantitatively. Figure 8 presents qualitatively pleasing images in accordance with the quantitative scores presented in the Table 1.

Figure 6 shows synthetic generation of underwater images for ocean water, and the corresponding restored results using the proposed conditional generative networks. Figure 7 shows synthetic generation of underwater images for coastal bed, and the corresponding restored results using the proposed conditional generative networks. Figure 5 depicts PSNR values for rendered synthetic underwater images against restored underwater images. PSNR estimates for ocean water and coastal beds depicts different behaviour representing the turbidity. It is evident from the quantitative metrics that, behaviour of water in ocean is significantly different from coastal beds.

6. Conclusions

In this work, we have presented a novel method for generating synthetic underwater images considering revised image formation model with depth as a clue. We have proposed to use the generated synthetic data to train conditional generative networks towards restoration of degraded underwater images. We show, underwater image formation model is sensitive to back scattering β_c^B, direct scattering β_c^D,and veiling light B_c^∞. We have demonstrated restoration of real underwater images through restoration framework trained using rendered synthetic underwater images, and have compared the results of restoration with state-of-the-art techniques using quantitative metrics.

7. Acknowledgement

This project is partly carried out under Department of Science and Technology (DST) through ICPS programme - Indian Heritage in Digital Space for the project "Digital Poompuhar" (DST/ ICPS/ Digital Poompuhar/ 2017 (General)).

References

[1] Derya Akkaynak and Tali Treibitz. A revised underwater image formation model. In *Proceedings of the IEEE Conference on Computer Vision and Pattern Recognition (CVPR)*, June 2018. 1, 2, 4

[2] Derya Akkaynak and Tali Treibitz. Sea-thru: A method for removing water from underwater images. In *Proceedings of the IEEE/CVF Conference on Computer Vision and Pattern Recognition (CVPR)*, June 2019. 4, 5

[3] D. Akkaynak, T. Treibitz, T. Shlesinger, Y. Loya, R. Tamir, and D. Iluz. What is the space of attenuation coefficients in underwater computer vision? In *2017 IEEE Conference on Computer Vision and Pattern Recognition (CVPR)*, pages 568–577, 2017. 3

[4] Raanan Fattal. Single image dehazing. *ACM Trans. Graph.*, 27(3):1–9, Aug. 2008. 2

[5] Clément Godard, Oisin Mac Aodha, Michael Firman, and Gabriel Brostow. Digging into self-supervised monocular depth estimation, 2019. 1

[6] Jinwei Gu, Jun Jiang, Sabine Susstrunk, and Dengyu Liu. What is the space of spectral sensitivity functions for digital color cameras? In *Proceedings of the 2013 IEEE Workshop on Applications of Computer Vision (WACV)*, WACV '13, page 168–179, USA, 2013. IEEE Computer Society. 4

[7] K. He, J. Sun, and X. Tang. Single image haze removal using dark channel prior. *IEEE Transactions on Pattern Analysis and Machine Intelligence*, 33(12):2341–2353, 2011. 2

[8] Deepti Hegde, Chaitra Desai, Ramesh Tabib, Ujwala B. Patil, Uma Mudenagudi, and Prabin Kumar Bora. Adaptive cubic spline interpolation in cielab color space for underwater image enhancement. *Procedia Computer Science*, 171:52–61, 2020. Third International Conference on Computing and Network Communications (CoCoNet'19). 7

[9] Leonhard Helminger, Michael Bernasconi, Abdelaziz Djelouah, Markus Gross, and Christopher Schroers. Blind image restoration with flow based priors, 2020. 2

[10] N.G. Jerlov. *Optical Oceanography*. ISSN. Elsevier Science, 2014. 3, 4, 6

[11] M. Johnson-Roberson, M. Bryson, B. Douillard, O. Pizarro, and S. B. Williams. Out-of-core efficient blending for underwater georeferenced textured 3d maps. In *2013 Fourth International Conference on Computing for Geospatial Research and Application*, pages 8–15, 2013. 1

[12] Matthew Johnson-Roberson, Mitch Bryson, Ariell Friedman, Oscar Pizarro, Giancarlo Troni, Paul Ozog, and Jon C. Henderson. High-resolution underwater robotic vision-based mapping and three-dimensional reconstruction for archaeology. *Journal of Field Robotics*, 34(4):625–643, 2017. 1

[13] Hiroharu Kato, Yoshitaka Ushiku, and Tatsuya Harada. Neural 3d mesh renderer, 2017. 1

[14] C. Li, C. Guo, W. Ren, R. Cong, J. Hou, S. Kwong, and D. Tao. An underwater image enhancement benchmark dataset and beyond. *IEEE Transactions on Image Processing*, 29:4376–4389, 2020. 7, 8

[15] C. Li, J. Quo, Y. Pang, S. Chen, and J. Wang. Single underwater image restoration by blue-green channels dehazing and

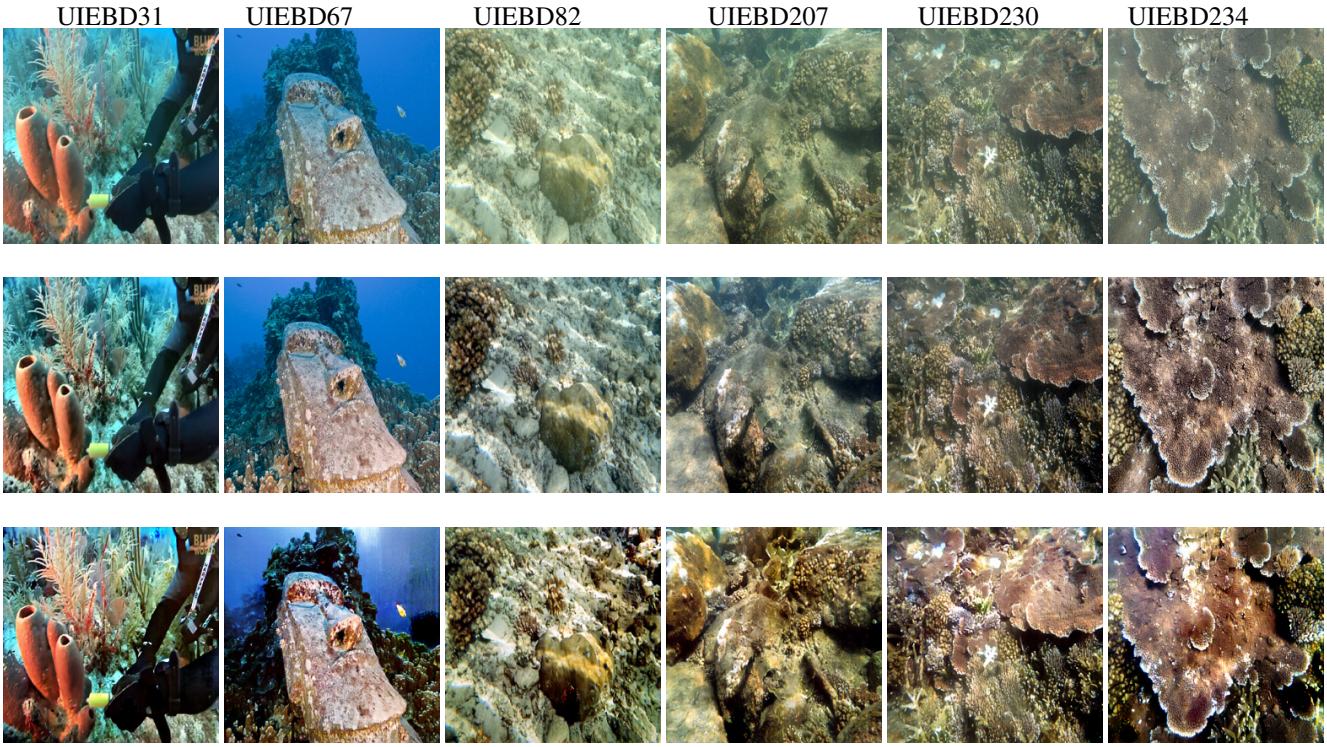

Figure 8. Restored underwater images using proposed methodology; First row corresponds to input images; Second row shows the restoration results of the authors in [14]; Third row shows the restoration results of our methodology. Quantitative evaluation for the same is shown in Table 1.

Table 1. Shows quantitative metrics (UCIQE [33], UIQM [22], and CCF [31]; " ↑ " indicates higher is better) of our method with the authors in [14]; Table depicts the quantitative scores computed using PUIQE [17] for the images depicted in Figure 8.

Dataset	UCIQUE			UIQM			CCF		
	Input	UIEBD	Ours	Input	UIEBD	Ours	Input	UIEBD	Ours
UIEBD31	0.62257	0.65194	**0.65902**	0.73003	0.83199	**0.85271**	29.91773	38.03104	**43.74388**
UIEBD67	0.55903	0.6286	**0.66718**	0.79573	0.91895	**0.92195**	33.41415	49.01754	**44.44922**
UIEBD82	0.46555	0.58044	**0.61096**	0.60523	0.68525	**0.7209**	23.38678	34.64003	**42.44393**
UIEBD207	0.49983	0.58104	**0.62572**	0.62868	0.7092	**0.73719**	22.02318	31.05702	**39.67916**
UIEBD230	0.5037	0.5787	**0.61568**	0.66417	0.71722	**0.74138**	21.36712	30.87587	**38.03149**
UIEBD234	0.45295	0.58906	**0.65134**	0.63976	0.71248	**0.83729**	19.30847	37.20978	**44.11102**

red channel correction. In *2016 IEEE International Conference on Acoustics, Speech and Signal Processing (ICASSP)*, pages 1731–1735, 2016. 3

[16] C. Li, J. Quo, Y. Pang, S. Chen, and J. Wang. Single underwater image restoration by blue-green channels dehazing and red channel correction. In *2016 IEEE International Conference on Acoustics, Speech and Signal Processing (ICASSP)*, pages 1731–1735, 2016. 3

[17] Chau Yi Li, Riccardo Mazzon, and Andrea Cavallaro. Underwater image filtering: methods, datasets and evaluation, Dec. 2020. 8

[18] Jie Li, Katherine A. Skinner, Ryan M. Eustice, and Matthew Johnson-Roberson. Watergan: Unsupervised generative network to enable real-time color correction of monocular underwater images. *CoRR*, abs/1702.07392, 2017. 2

[19] Mehdi Mirza and Simon Osindero. Conditional generative adversarial nets, 2014. 2

[20] U. Mudenagudi and S. Ghaudhuri. Depth estimation using defocused stereo image pairs. In *Proceedings of the Seventh IEEE International Conference on Computer Vision*, volume 1, pages 483–488 vol.1, 1999. 2

[21] Pushmeet Kohli Nathan Silberman, Derek Hoiem and Rob Fergus. Indoor segmentation and support inference from rgbd images. In *ECCV*, 2012. 4

[22] K. Panetta, C. Gao, and S. Agaian. Human-visual-system-inspired underwater image quality measures. *IEEE Journal of Oceanic Engineering*, 41(3):541–551, 2016. 7, 8

[23] Zeba Patel, Chaitra Desai, Ramesh Ashok Tabib, Medha Bhat, Ujwala Patil, and Uma Mudengudi. Framework for underwater image enhancement. *Procedia Computer Sci-*

ence, 171:491–497, 2020. Third International Conference on Computing and Network Communications (CoCoNet'19). 7

[24] Ujwala Patil, Uma Mudengudi, K. Ganesh, and Ravikiran Patil. Image fusion framework. In Vinu V. Das, Janahanlal Stephen, and Yogesh Chaba, editors, *Computer Networks and Information Technologies*, pages 653–657, Berlin, Heidelberg, 2011. Springer Berlin Heidelberg. 7

[25] Ujwala Patil, Ramesh Ashok Tabib, Rohan Raju Dhanakshirur, and Uma Mudenagudi. Evidence-based image registration and its effect on image fusion. In Atilla Elçi, Pankaj Kumar Sa, Chirag N. Modi, Gustavo Olague, Manmath N. Sahoo, and Sambit Bakshi, editors, *Smart Computing Paradigms: New Progresses and Challenges*, pages 29–39, Singapore, 2020. Springer Singapore. 7

[26] Ujwala Patil, Ramesh Ashok Tabib, Channabasappa M. Konin, and Uma Mudenagudi. Evidence-based framework for multi-image super-resolution. In Pankaj Kumar Sa, Sambit Bakshi, Ioannis K. Hatzilygeroudis, and Manmath Narayan Sahoo, editors, *Recent Findings in Intelligent Computing Techniques*, pages 413–423, Singapore, 2018. Springer Singapore. 7

[27] Olaf Ronneberger, Philipp Fischer, and Thomas Brox. U-net: Convolutional networks for biomedical image segmentation. *CoRR*, abs/1505.04597, 2015. 5

[28] Y. Y. Schechner and N. Karpel. Clear underwater vision. In *Proceedings of the 2004 IEEE Computer Society Conference on Computer Vision and Pattern Recognition, 2004. CVPR 2004.*, volume 1, pages I–I, 2004. 3

[29] Michael G. Solonenko and Curtis D. Mobley. Inherent optical properties of jerlov water types. *Appl. Opt.*, 54(17):5392–5401, Jun 2015. 2, 4

[30] Robby T. Tan. Visibility in bad weather from a single image. *2008 IEEE Conference on Computer Vision and Pattern Recognition*, pages 1–8, 2008. 2

[31] Yan Wang, Na Li, Zongying Li, Zhaorui Gu, Haiyong Zheng, Bing Zheng, and Mengnan Sun. An imaging-inspired no-reference underwater color image quality assessment metric. *Computers & Electrical Engineering*, 70:904–913, 2018. 7, 8

[32] Y. Wang, H. Liu, and L. Chau. Single underwater image restoration using attenuation-curve prior. In *2017 IEEE International Symposium on Circuits and Systems (ISCAS)*, pages 1–4, 2017. 2

[33] M. Yang and A. Sowmya. An underwater color image quality evaluation metric. *IEEE Transactions on Image Processing*, 24(12):6062–6071, 2015. 7, 8